Journal of Computers Vol. 30 No. 1, 2019, pp. 75-86
doi:10.3966/199115992019023001008

A Robust Fusing Strategy for Respiratory Rate Estimation From Photoplethysmography Signals

Chi-Keng Wu[1], Pau-Choo Chung[2*]

[1] Department of Electrical Engineering, National Cheng Kung University, Tainan 701, Taiwan, ROC
inchrist.chikeng@gmail.com

[2] Department of Electrical Engineering, National Cheng Kung University, Tainan 701, Taiwan, ROC
pcchung@ee.ncku.edu.tw

Received 9 January 2018; Revised 22 January 2018; Accepted 22 January 2018

Abstract. Respiratory rate (RR) estimation using Photoplethysmogram (PPG) signals has the advantage of high usability and wearability. However PPG sensor is very sensitive to motion artifacts, resulting that the RR features derived from the four respiratory-induced variations (intensity, frequency, amplitude and pulse width) of PPG may present significant inconsistency values. To address this problem, we propose an adaptive fusion approach based on Kalman Filter (KF) to adaptively fuse the RR features in the PPG signals. The model applies the relationship of inter-feature coherence and intra-feature statistical changes to identify the measurement process and the four RR state processes of the KF for the four variations intensity, frequency, amplitude and pulse width, respectively. The fusion of the four estimated RRs from state space of the KF is performed according to the instant Kalman gain and feature consistency metric. The experimental results of 42 subjects show that the proposed adaptive fusion model can effectively improve the estimation accuracy, especially when the four RR features are significantly diverse.

Keywords: adaptive fusion, Kalman filter (KF), photoplethysmography (PPG), respiratory rate (RR)

1 Introduction

Ambulatory monitoring of respiratory rate (RR) has the advantage of long-term state-of-health (e.g. patient care) monitoring [1]. Recently, it has been found that RR can be used for mental state recognition, such as depression, stress and emotional states [2-3]. Photoplethysmography (PPG) measures the pulse wave caused by periodic pulsations in arterial blood volume by infrared light-emitting diodes and photo detectors. Non-invasive, high availability and low cost, making it a popular sensor kit for portable devices. PPG is widely used to heart rate monitor and is gradually validated to contain various respiratory-modulated signals which can be used for respiratory activity monitoring [4-8]. Respiration has been exploited to modulate the PPG in several ways: Respiratory sinus arrhythmia (RSA) phenomenon will lead to respiratory-induced frequency variation (RIFV) in the PPG signal. The variation of intrapleural pressure causing the exchange of blood circulation results in respiratory-induced intensity variation (RIIV). Beside, the decrease in cardiac output influences the change of peripheral pulse strength and causes the respiratory-induced amplitude variation (RIAV). In [9], the relationships between respiratory rate and the three respiratory-induced variations (called RR variations) in PPG were investigated and compared. Combining these RR variations to improve accuracy for respiratory rate estimation has also been validated. For instances, Johansson [10] combined the three RR variations using feed-forward neural network model to monitor RR. While PPG signals record using pulse oximetry, the interaction of Infrared light with biological tissue can be quite complex and may involve scattering absorption and reflection [11]. If the recording data involved in physical motion artifacts, it will result in

* Corresponding Author

strong baseline drift or distortion, and unable to be restored effectively. In practical, the pulse wave morphology is completely superimposed by disturbances or distorted caused by incomplete signal reception, causing it impossible to restore. While it is almost impossible to remove the motion artifacts (MAs), many recent algorithms choose to neglect the low signal quality segments [12-14], and the RR estimations were performed only on good-quality segments. In general, accurate RR estimates from short PPG segments has been well-validated. However, practical applications require long-term ambulatory monitoring. In this case, MAs are inevitable. Therefore, recent challenge is on the robust RR estimation in the presence of MAs. To address such an impending demand, several algorithms have been proposed based on finding a more robust approach for combining respiratory modulate information in PPG. The approach in [12] is to find the most trustful intervals during PPG recording so that mean fusion of the three RR variations (RIIV, RIAV, RIFV) can be utilized to enhance RR estimation accuracy. Their approach first discards the low signal quality intervals (artifacts), and then neglect the windows in which the standard deviation among the three variations is higher than 4. However, the occurrence of the latter is very high causing most of the windows are removed (totally 45.5%). Accordingly the output will be strongly discontinuous. The approach in [14] utilizes multiple autoregressive models (based on Burg's algorithm) with different model orders to estimate the dominated frequency among the three RR variations to estimate RR. The idea is to find the most reliable RR estimate in the three RR variations within a relatively good signal quality window (about 10% data are discarded). However, by using this method, there are 3×17 AR models need to be estimated within a window. If the overlapping ratio of sliding window is high, such approach will be very time consuming. Besides, as discussed in [14], different window sizes used for estimating RR can result in substantially different accuracy levels.

In this study, we proposed an adaptive fusion approach based on Kalman Filter (KF) to dynamically fuse four RR feature sequences according to their inter- and intra- characteristic relationships for robust RR estimation. The four RR feature sequences are derived from four RR variations which extracted from pulsatile component of PPG waveform. The four RR variations include the three variations (RIFV, RIIV, and RIAV), that are commonly used in the literatures (e.g. [12, 14]), and a PPG pulse width based variation (PWV) [15]. MAs in PPG signal would raise the deviation level between feature sequences and distorted physiological response within each feature sequence. Moreover, different feature sequences may be subject to different levels of abnormal disturbance.

Suppose there are several feature time series in the system. And there is a sequence formed by inter-feature relationship, and another sequence describes the changes/variation state of a feature (intra-feature variation). Let both sequences be the measurement and state process of a KF, respectively. The KF can adaptively control the process state by minimizing the error covariance from state and measurement sequence. Blending factor of the filter will be reveled in the Kalman gain, which can be used to understand how strong the priori estimated state maintains the control process so as to obtain the instant quality of the intra-feature in state process corresponding to measurement (inter-feature). By this concept, the state (controlled) space of the KF is formulated to describe the models of the RR feature sequences according to each intra-feature variation. The measurement process of the KF is the coherence state of the four RR features. While the four RR features are highly consistent, this implies RR values in these features are reliable. Then the mean fusion is employed to fuse the four estimated RR in state space, however, if the four features present inconsistence, the filter will find the most trustful estimated RR in state space through Kalman gain. To address the problem of severe distortion data, the PPG pulse waves which detected having low signal quality are eliminated from the accuracy evaluation.

The rest of this paper is structured as follows. Section 2 describes the preprocessing of PPG signal including PPG pulse segmentation and RR feature extraction. Section 3 introduces the algorithm designed to adaptive fuse the four RR features to provide improved robustness of RR estimation. The experiment data are described in Section 4. The evaluation of our method and comparison are discussed in Section 5. Finally, we presented the conclusion in Section 6.

2 Preprocessing of PPG Signal

2.1 PPG Pulse Segmentation

The PPG signal consists of DC component and pulsatile component (AC). To extract the AC component, a Low-Pass Filter with $f_c = 8$ Hz is applied to obtain a smoothed PPG signal. Then a Low-Pass Filter

with $f_c = 0.5$ Hz is applied to estimate the DC trend. The pulsatile AC component S_t is then obtained by subtracting the DC trend from the smoothed PPG signal. Subsequently, a pulse segmentation procedure is applied to partition each of the pulse waves from S_t. The procedure is based on detecting the rising edge of each pulse wave(e.g. [16, 18]), as follows:

- Find the zero crossing points in the first-order derivative of S_t, denoted as p_i.
- The interval between point p_{i-1} and p_i is accepted as a rising period of a pulse wave, if in the conditions that $S_{p_{i-1}} \le 0$ and $S_{p_i} > 0$, the intensity of the rising edge is larger than a certain percent of the moving average of the pulse wave intensity.

2.2 Respiratory Rate Feature Extraction

Four respiratory-induced variations (RIFV, RIIV, RIAV, and PWV) from PPG signals are extracted in the computing of respiratory rate. Let the time points of onset and peak of the *i*-th PPG pulse waves be denoted as the pairs $\{t_{o,i}, t_{p,i}\}_{i=1,\ldots N}$, and the correspond value denoted as $\{S_{t_{o,i}}, S_{t_{p,i}}\}_{i=1,\ldots N}$. The four respiratory-induced variations are defined as

$\mathrm{RIFV}_i = t_{p,i} - t_{p,i-1}$,

$\mathrm{RIIV}_i = S_{t_{p,i}}$,

$\mathrm{RIAV}_i = S_{t_{p,i}} - S_{t_{o,i}}$,

and $\mathrm{PWV}_i = t_{o,i} - t_{o,i-1}$.

The resulting four time-series are then resampled to original sample rate (referred to as a tachogram). In this study, RR is estimated using instant respiration rate estimation derived from each respiratory cycle in the four variations. The advantage of using instant RR estimation is that the coherence between respiration and PPG derived signal can be compared cycle by cycle [17]. As such, the effect of window size can be prevented [18]. To estimate instant RR features, a band pass filter is applied to the four tachograms. Then the valley-peak pairs can be extracted as the procedures described in Section 2.1. After the valley-peak pairs detected, the instant RR feature sequences can be estimated by calculating the distance between adjacent peaks. Since the normal range of adult breathing rates is between 0 and 60 breath/minute, the four derived RR feature sequences are then interpolated (and resampled) at 1 Hz, [19]. The results from the four derived RR feature sequences are denoted as R_n^W, R_n^I, R_n^A and R_n^F, respectively. Besides, in order to estimate motion artifact effect, we further estimate the instant valley to peak distance from above detected valley-peak pairs, referred to as the amplitude varying activity in the four RR variations and denoted as A_n^W, A_n^I, A_n^A, A_n^F.

3 Adaptive Filter for RR feature Fusion

3.1 Process Model Description

Let us assume that the four RR feature sequences are dynamic system with a process model (also called control process) as following

$$\mathbf{x}_n = \Phi \mathbf{x}_{n-1} + \mathbf{u}_{n-1} + \mathbf{w}_n, \tag{1}$$

and only a noisy linear combination $\mathbf{\Pi}$ of the system states

$$\mathbf{z}_n = \mathbf{\Pi} \mathbf{x}_n + \mathbf{v}_n \tag{2}$$

can be measured. The $\mathbf{x}_{n-1}$ here is the state vector representing the estimated RR at the previous time step $n-1$ which with a state transition matrix Φ relates to the current state $\mathbf{x}_n$. $\mathbf{u}_{n-1}$ is the control input to the state $\mathbf{x}_n$, which is the increase rate of RR. Let $\mathbf{Q}_n = E\left[\mathbf{w}_n \mathbf{w}_n^T\right]$ and $\mathbf{R}_n = E\left[\mathbf{v}_n \mathbf{v}_n^T\right]$ be the process noise covariance and measurement noise covariance, respectively. The goal of KF is to produce the optimal estimate $\hat{\mathbf{x}}_n$ of $\mathbf{x}_n$ that is corrected for the measurement $\mathbf{z}_n$. The state space is formulated from

the four instant RR features. Thus, the input vector $\mathbf{u}_{n-1}$ is the increase rate of RR from the four RR features, R_n^W, R_n^I, R_n^A, R_n^F, defined as

$$\mathbf{u}_{n-1} = \begin{bmatrix} R_n^W - R_{n-1}^W \\ R_n^I - R_{n-1}^I \\ R_n^A - R_{n-1}^A \\ R_n^F - R_{n-1}^F \end{bmatrix}. \tag{3}$$

Φ in (1) is a 4×4 identity matrix, which assume there is no state transition correction. Assuming that in the ideal condition, the state estimates have the vector form $\mathbf{x}_n = \left[R_n^W, R_n^I, R_n^A, R_n^F \right]^T$.

When the four respiratory-induced variations are disturbed by motion artifact, the noise covariance, $\mathbf{Q}_n$, in the state process will be raised. Since the disturbance may affect the signal frequency and amplitude variance, $\mathbf{Q}_n$ can be estimated by calculating the instant frequency/amplitude change, the brief procedures are depicted in Fig. 1. Let $\{\delta R_n^\ell\}$ and $\{\delta A_n^\ell\}$ be sequence of the estimated change rates with respect to the frequency and amplitude of the respiratory-induced variation, respectively, $\ell \in \{W, I, A, F\}$, defined as

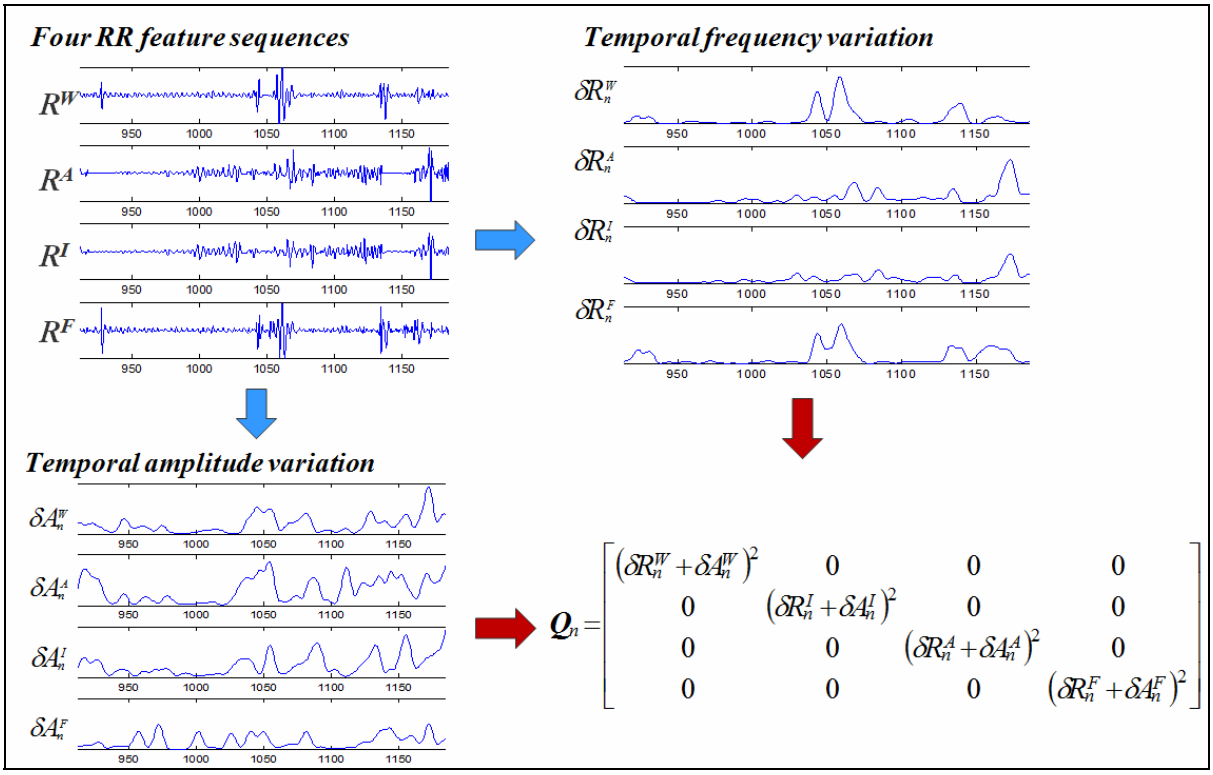

Fig. 1. The procedure of process noise covariance $\boldsymbol{Q}_n$ estimation

$$\delta R_n^\ell = H\left(\Delta R_n^\ell\right) \text{ where } \Delta R_n^\ell = \left| R_n^\ell - R_{n-1}^\ell \right| \tag{4}$$

$$\delta A_n^\ell = H\left(\Delta A_n^\ell\right) \text{ where } \Delta A_n^\ell = \left| A_n^\ell - A_{n-1}^\ell \right| \tag{5}$$

where $H(.)$ is the convolution operator which convolute sequence $\{\Delta R_n^\ell\}$ and $\{\Delta A_n^\ell\}$ with Hanning window function,

$$\omega(\kappa) = \sin^2\left(\frac{\pi\kappa}{11}\right), \tag{6}$$

Where $\kappa = 0,1,...,11$. Assuming that the features are independent of each other, the process noise covariance matrix of the state process can be defined as

$$\mathbf{Q}_n = \begin{bmatrix} \left(\delta R_n^W + \delta A_n^W\right)^2 & 0 & 0 & 0 \\ 0 & \left(\delta R_n^I + \delta A_n^I\right)^2 & 0 & 0 \\ 0 & 0 & \left(\delta R_n^A + \delta A_n^A\right)^2 & 0 \\ 0 & 0 & 0 & \left(\delta R_n^F + \delta A_n^F\right)^2 \end{bmatrix}. \tag{7}$$

If the four RR features have the same values or are extremely consistent in the high PPG signal quality interval, the mean value of the four RR features should be very close to *real* **RR**. Thus, the measurement $\mathbf{z}_n$ of the KF can be defined as

$$\mathbf{z}_n \cong \frac{1}{4}\sum_{\kappa} R_n^{\ell}, \ if \ Var\left[R_n^{\ell}\right] \cong 0, \ \ell \in \{W, I, A, F\}. \tag{8}$$

As such, the relation matrix $\mathbf{\Pi}$ between $\mathbf{x}_n$ and $\mathbf{z}_n$ can be formed as a constant matrix in the ideal condition ($\mathbf{v}_n = \mathbf{0}$):

$$\mathbf{\Pi} = [0.25, 0.25, 0.25, 0.25], \text{ and } \mathbf{z}_n = \mathbf{\Pi}\mathbf{x}_n. \tag{9}$$

If the value of $Var\left[R_n^{\ell}\right]$ is large, implying that respiratory rate among the four features are significantly inconsistent, $\mathbf{z}_n$ will lose its representative as the *real* measurement. Accordingly, the measurement noise covariance of the KF can be defined as

$$\mathbf{R}_n = \left[Rdv_n\right]^2, \tag{10}$$

and the variance metric is

$$Rdv_n = \frac{1}{4}\sum_{\ell}\left(\tilde{R}_n^{\ell} - \mu_{\tilde{R}_n}\right), \ \ell \in \{W, I, A, F\} \tag{11}$$

where $\mu_{\tilde{R}_n}$ is the mean value of the $\tilde{R}_n^{\ell}$. $\tilde{R}_n^{\ell}$ is the normalized value of R_n^{ℓ} and is normalized to [0, 1], corresponding to RR range between 4Hz to 60 Hz. The obtained Rdv_n has the value between 0 and 0.5.

3.2 Update Equations

The time update equation of error covariance is

$$\mathbf{P}_n^{-} = \mathbf{P}_{n-1} + \mathbf{\Gamma}\mathbf{Q}_n\mathbf{\Gamma}^T, \tag{12}$$

where $\mathbf{P}_n$ is the error covariance matrix. $\mathbf{\Gamma}$ is a diagonal matrix, where the diagonal elements are the constant scale factor associating with the process noise covariance $\mathbf{Q}_n$. The Kalman gain matrix, $\mathbf{K}_n$, is computed by

$$\mathbf{K}_n = \frac{\mathbf{P}_n^{-}\mathbf{\Pi}^T}{\mathbf{\Pi}\mathbf{P}_n\mathbf{\Pi}^T + \mathbf{V}\mathbf{R}_n\mathbf{V}^T}, \tag{13}$$

where $\mathbf{K}_n = [K_n^W, K_n^I, K_n^A, K_n^F]^T$. $\mathbf{V}$ is a diagonal matrix, and the diagonal elements are the constant scale factor associating with the measurement noise covariance $\mathbf{R}_n$. While the a priori estimate is predicted ($\hat{\mathbf{x}}_n^{-} = \hat{\mathbf{x}}_{n-1} + \mathbf{u}_{n-1}$), the measurement innovation is given as

$$\gamma_n = \mathbf{z}_n - \mathbf{\Pi}\hat{\mathbf{x}}_n^- . \tag{14}$$

Subsequently, the a priori estimate and error covariance are corrected by

$$\hat{\mathbf{x}}_n = \hat{\mathbf{x}}_n^- + \mathbf{K}_n\gamma_n , \tag{15}$$

$$\mathbf{P}_n = \mathbf{P}_n^-(\mathbf{I} - \mathbf{K}_n\mathbf{\Pi})^T . \tag{16}$$

3.3 Fusion Policy and RR Estimation

The fusion policy is based on the temporal coherence of the four RR variations. While the four RR features have high consistency, it involves that four estimated RR features in $\hat{\mathbf{x}}_n$ are very close. In this condition when $Rdv_n \le Th_{Rdv}$, the final RR estimation is calculated by

$$RR_n = mean(\hat{\mathbf{x}}_n) , \tag{17}$$

where Th_{Rdv} is the experience threshold value to determine the consistency quality of Rdv_n. However, if the four RR features are divergence ($Rdv_n > Th_{Rdv}$), the measurement noise covariance will be high. The Kalman gain will adjust the filter tend to more "trust" a prior estimate of state process. Since the disturbances in the four features are different, resulting in different a posteriori estimated RR results in state space. In this condition, the "fusion" is to find the best estimated feature in state space. According to (12) and (13), the state in state space with relative low noise interference (refer to (6)) will obtain lower Kalman gain value. Such relationship is used to determine the most trustful estimated RR feature among $\hat{x}_n^\ell$ as the final RR estimation, that is

$$RR_n = \hat{x}_n^{\ell^*} , \tag{18}$$

where

$$\ell^* = \arg\min_{\ell} \left\{ K_n^\ell \right\}, \ \ell \in \{W, I, A, F\} . \tag{19}$$

4 Experimental Data

PPG data set were acquired from 46 healthy adults. For four of these subjects, the reference respiration was invalid in most portions due to measurement deviation by sensor displacement. The durations of available data recorded from 42 subjects are each between 70min~86min. During the experiment, a pulse oximeter attached to the subject's left hand. The reference respiration signal (ground truth) was acquired via an elasticized gauge attached circumferentially around the subject's chest [3, 21]. In order to obtain respiratory activity data just like daily life, the subjects were asked to watch several emotional movies [3], to speak and interact with a computer, and to move body or swung hand. Fig. 2 shows the recorded PPG of a subject containing motion artifacts with a strong baseline wander (DC component shift).

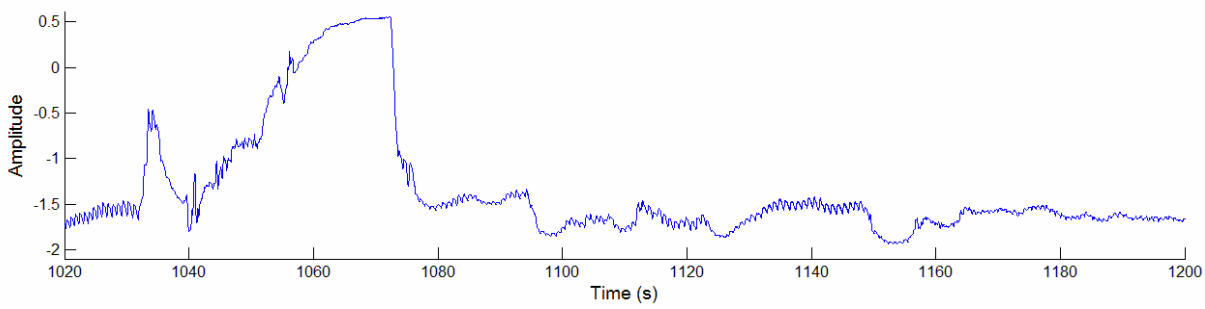

Fig. 2. The recorded PPG containing motion artifacts with a strong baseline wander (3 minutes of data)

5 Results and Discussion

5.1 Signal Quality Metric

To identify artificial and low-quality periods of the PPG signals, a modified version of [20] is used to estimate PPG wave signal quality (SQ). The steps involve in estimating SQ of PPG pulse waves are described as follows:

Step 1: Benchmark Estimation

Calculate the squared value of the first-order derivative for each PPG pulse wave.

- Calculate the average wave length of all pulse waves in long-term data, denoted as *L*. Subsequently, resample each pulse wave into fixed length *L*.
- Align each pulse wave by subtracting its onset point value.
- Estimate the median pulse wave from all the pulses of the individual data as the benchmark waveform, denoted as $\bar{\chi}_k$.

Step 2: Estimate signal quality for each PPG pulse wave

- The cross correlation coefficient criterion is used to matching of the benchmark with all of the pulse waves:

$$SQ_i = \sum_{k=1}^{L} \hat{\chi}_k^i \cdot \bar{\chi}_k \left(\sum_{k=1}^{L} \left(\hat{\chi}_k^i \right)^2 \cdot \sum_{k=1}^{L} \left(\bar{\chi}_k \right)^2 \right)^{-1/2} \tag{20}$$

where $\hat{\chi}_k^i$ denotes the *i*-th pulse wave. If $SQ_i < Th_{SQ}$, the pulse wave is considered of low quality, where Th_{SQ} is an experience threshold.

5.2 Evaluation

In long-term monitoring, it is inevitable to contain disturbed intervals in the reference respiratory signals. To obtain the ground truth data for performance comparison, we applied the method introduced in Section 5.1 to measure the quality of the reference respiration signal collected from elasticized gauge. The quality is denoted as SQ_n^{resp} . The respiration waveform with $SQ_n^{resp} \geq 0.85$ is considered to be the ground truth. As a result a total of 15.4% data ($SQ_n^{resp} < 0.85$) in our database has been excluded from accuracy evaluation. The low quality PPG signal intervals (SQ<0.85) are also neglect (8.4% in average).

The obtained RR estimation is compared with the reference RR. The performance was assessed by calculating the mean absolute error (MAE) in breaths/min and is defined as

$$MAE_n = \frac{1}{N} \sum_{n=1}^{N} \left| \mathrm{RR}_n^{ref} - \mathrm{RR}_n^{alg} \right| . \tag{21}$$

The RR estimation performance of the proposed model was compared with that obtained using mean [12] and median fusion, and another window based fusion method (referred to AR-fusion in the paper) in [14] which has been introduced in Section 1. In order to make a fair comparison with the AR-fusion algorithm, the window size for AR model is set as 15 seconds (4 breaths/min), with 1sec shift [19]. With the 15 second window size, there are possibly 1~15 breath cycles for a healthy adult. In order to achieve the same comparison criteria, the dominant frequency within the window from reference respiratory signal is used as the ground truth of RR. Since our method uses four RR variations, the AR-fusion method was implemented with both three variations (without PWV) and four variations (with PWV), respectively. Furthermore, the accuracy is calculated when the PPG $SQ > 0.85$ and ground truth available.

5.2 Results and Discussion

Fig. 3(a) shows the RR estimation results obtained for a 400-second PPG segment using proposed model and mean fusion approach. The corresponding values of Rdv_n , SQ_n and SQ_n^{resp} are shown in Fig. 3(b) to

Fig. 3(d). Consider in the high signal quality interval, when Rdv_n is small which will involve with small $\mathbf{R}_n$ in the KF. This implies that the four RR features appear to have close values, resulting in similar value in diagonal elements of $\mathbf{Q}_n$. It can be seen that in Fig. 3(a), the final RR estimation of the filter (mean value of the four estimated RR features) is very close to the result of mean fusion.

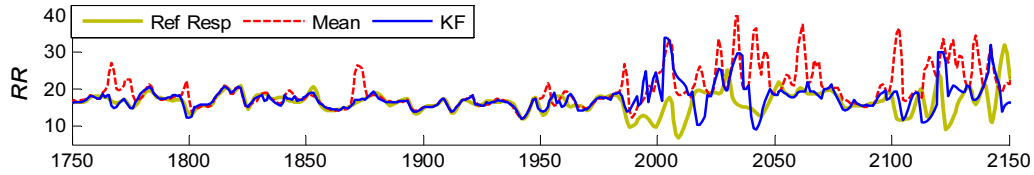

(a) Comparison of KF model, mean value of the four RR features, and reference respiration, respecitvely

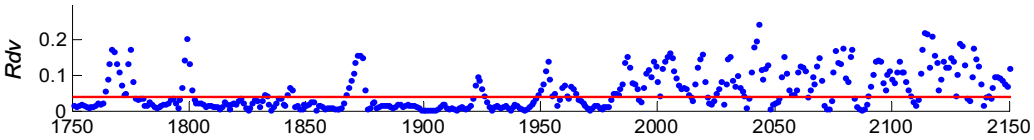

(b) Variation feature consistency (Rdv_n)values

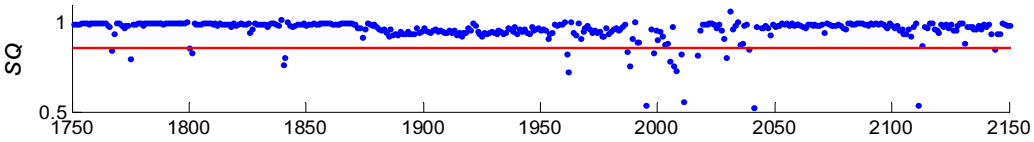

(c) SQ_n values of PPG signal

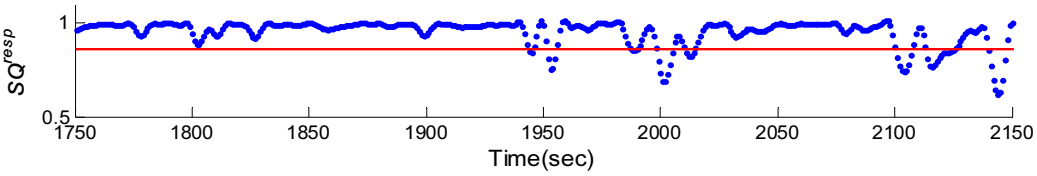

(d) SQ values of reference respiration
The red lines in (b), (c), (d) indicate the corresponding threshold values

Fig. 3. The results for a 400-second PPG segment

As described in (13), Kalman gain is adjusted by $\mathbf{R}_n$ and $\mathbf{P}_n$. In our modal, we assume that the relationship between states *n* and *n-1* does not change with time ($\mathbf{A} = I$). Accordingly $\mathbf{P}_n$ will be directly affected by $\mathbf{Q}_n$. When the value of $\mathbf{R}_n$ becomes larger (affected by Rdv_n), the element of Kalman gain vector will adjust depending on the instant frequency/amplitude change of the corresponding respiratory-induced variations. For instance, when Rdv_n becomes larger and the instant activities of PWV is relatively small, this implies that PWV may be subjected to relatively small disturbed. As such, there is relatively small $\left(\delta R_n^W + \delta A_n^W\right)^2$ value in $\mathbf{Q}_n$, which results in relative small K_n^W value in $\mathbf{K}_n$. If K_n^W is the smallest value in $\mathbf{K}_n$, the corresponding estimated RR feature $\hat{x}_n^W$ will be selected as final RR estimation.

In order to investigate the fusion performance, Fig. 4(a) and Fig. 5(a) show the results of RR estimation from the four features, mean fusion, KF fusion, and reference signal. It can be seen that even

if the signal has a high *SQ* (>0.85), as shown in Fig. 4(b) and Fig. 5(b), the four features are still significantly different. By using our fusion approach, the filter in most of the time can achieve highly accurate estimate (shown in blue dotted line) compared to the mean fusion (red dotted line). As can be seen from these figures, if the four RR features are all far from the ground truth, the proposed method cannot effectively reduce the error. This is because that our approach is to find the best estimated RR feature in state space as the representative. This is the limitation of our method.

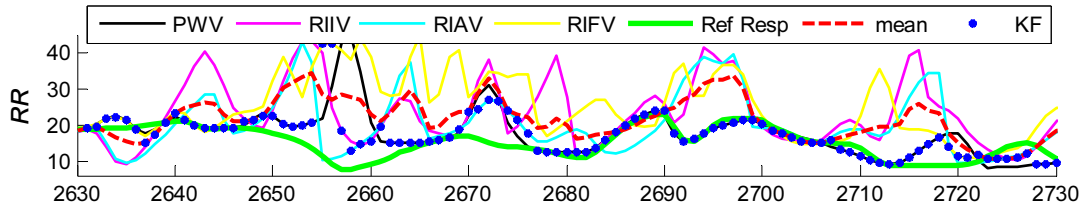

(a) The RR estimates from four features, mean fusion, KF fusion, and reference respiratory, respectively

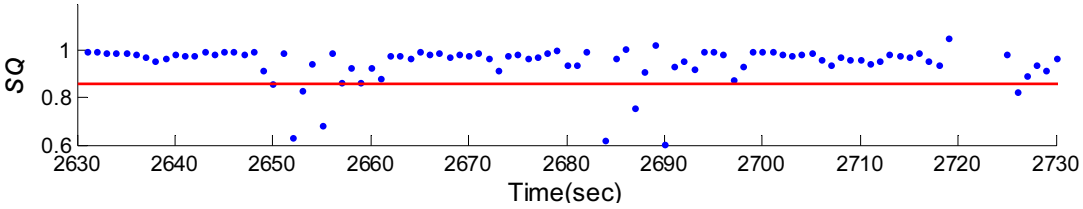

(b) corresponding SQ

Fig. 4. The RR estimation results for a 100-second interval of subject#02

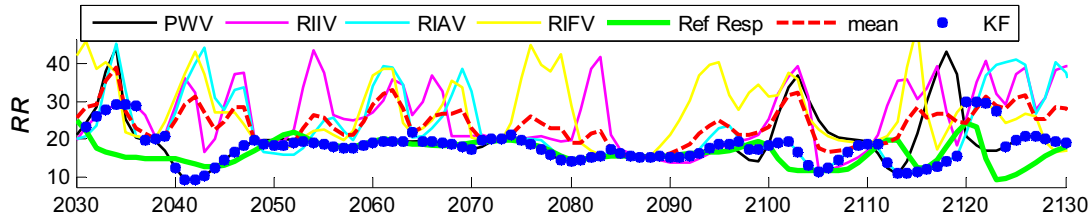

(a)

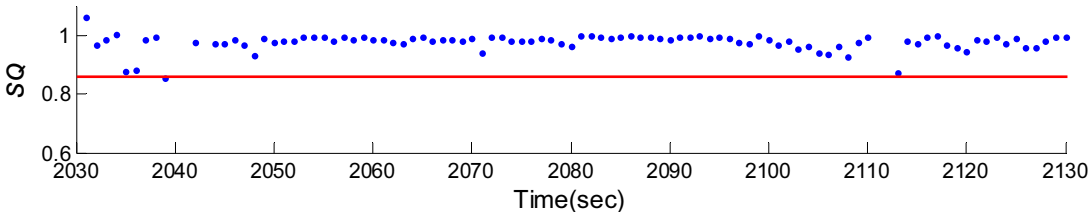

(b)

Fig. 5. The RR estimation results for a 100-second interval of subject#02

Table 1 shows the comparison result of the MAE performance for 42 subjects. The mean value using our method is 3.12 breaths/min, which is superior to the other three fusion methods (mean, median, AR-fusion). It also has the lowest maximum error 4.12 breaths/min and minimum error 1.87 breaths/min. Table 1 also shows that, regardless of which fusion method is used, the estimation results of respiratory rate among subjects are very different. The minimum MAE obtained using our method comes to 1.87 breaths/min and the maximum is 4.12 breaths/min.

Table 1. Performance of each fusion algorithm individually using mean absolute error (MAE)

	Fusion methods (MAE)						Respiratory-induced variations (MAE)			
Subj.	**KF**	**Median**	**Mean (4)****	**Mean (3)***	**AR (4)****	**AR(3)***	**PWV**	**RIIV**	**RIAV**	**RIFV**
01	**4.04**	7.46	8.43	10.17	5.33	6.31	4.24	12.98	7.62	10.92
02	**2.14**	3.01	3.39	3.99	2.67	3.16	2.59	4.97	3.77	5.00
03	3.26	3.72	3.94	4.20	**3.04**	3.23	3.90	5.29	3.97	4.92
04	**4.12**	5.90	6.69	7.87	5.96	6.97	4.44	11.43	7.49	6.92
05	**4.01**	4.30	4.38	4.55	4.93	5.24	4.64	5.71	4.84	4.98
06	2.04	**2.02**	2.14	2.41	2.13	2.40	2.22	3.81	2.80	2.77
07	**3.62**	4.91	5.56	6.47	4.05	5.09	4.13	10.03	5.97	6.21
08	4.11	**3.91**	4.19	4.75	4.90	5.67	4.32	8.61	5.65	4.52
09	**3.26**	3.72	3.94	4.20	3.04	3.23	3.90	5.29	3.97	4.92
10	**3.88**	4.09	4.17	4.52	3.71	4.47	4.11	6.23	5.22	4.73
11	4.10	4.55	4.67	5.24	**3.78**	4.97	4.42	6.81	5.45	6.84
12	**2.38**	3.69	4.62	5.53	2.65	3.92	3.10	9.16	4.70	4.70
13	**2.59**	3.20	3.50	4.05	2.49	3.22	2.95	5.83	3.90	4.58
14	**3.97**	5.57	6.19	7.23	4.60	5.37	4.13	8.93	6.26	8.43
15	**1.93**	2.20	2.37	2.60	1.90	2.28	2.43	4.19	2.77	2.84
16	**3.82**	4.98	5.42	6.05	4.44	4.79	4.63	8.26	5.71	6.40
17	3.88	**3.68**	3.70	4.05	3.87	5.14	3.89	5.61	5.23	4.61
18	**2.59**	3.53	4.20	4.87	3.40	4.07	3.08	7.68	4.40	4.31
19	**3.63**	4.48	4.78	5.53	4.18	5.02	3.94	7.41	5.45	6.09
20	**2.59**	3.58	4.01	4.72	2.95	3.61	3.11	6.67	4.64	5.10
21	**3.37**	3.96	4.23	4.77	3.52	3.99	3.61	6.67	4.96	4.76
22	**4.00**	4.90	5.40	6.20	3.86	4.86	4.70	7.82	5.69	7.94
23	**3.23**	4.21	4.51	5.40	3.75	4.37	**3.23**	6.60	5.15	6.74
24	**3.91**	5.80	6.49	7.44	4.74	5.57	4.85	10.78	6.40	7.34
25	**2.78**	2.75	3.03	3.43	2.83	3.34	3.12	5.20	3.59	4.27
26	**2.72**	2.98	3.28	3.85	3.25	4.00	2.85	5.50	4.07	4.88
27	**2.85**	3.70	4.02	4.51	3.17	3.32	3.29	5.29	4.22	5.39
28	**2.09**	2.67	2.96	3.46	2.19	2.71	2.38	4.03	3.52	4.80
29	**3.19**	4.18	4.59	5.28	3.84	4.28	3.58	6.05	4.49	7.06
30	**2.11**	2.71	3.13	3.57	2.37	2.61	2.56	5.32	3.18	3.74
31	**2.65**	3.53	3.79	4.18	2.96	3.08	3.72	4.61	3.94	5.65
32	**2.77**	5.13	6.14	7.58	3.83	5.11	3.02	9.55	5.66	9.14
33	2.25	2.61	3.05	3.50	**2.10**	2.32	2.81	3.80	3.21	5.40
34	**3.53**	4.00	4.15	4.55	3.80	4.60	3.92	6.04	4.93	5.03
35	**3.39**	3.44	3.61	4.04	4.60	4.85	3.70	6.58	4.55	3.94
36	**2.44**	3.46	4.01	4.64	2.95	3.55	2.95	6.27	3.84	5.26
37	2.98	4.16	4.74	5.43	**2.83**	3.31	3.53	7.33	4.79	5.83
38	**2.48**	3.52	3.96	4.33	3.04	3.14	3.56	5.06	3.71	5.73
39	**2.56**	3.84	4.77	5.77	3.61	4.22	3.04	8.37	4.88	6.23
40	4.00	3.23	3.42	3.93	**2.65**	7.11	3.07	6.00	4.25	5.00
41	3.86	3.67	3.77	4.22	**3.26**	3.81	3.63	5.74	4.85	5.22
42	**1.87**	2.41	2.86	3.33	1.89	2.28	2.32	4.26	2.88	4.71
Mean	**3.12**	3.89	4.29	4.91	3.45	4.16	3.51	6.71	4.68	5.57
ST.D.	0.72	1.06	1.21	1.49	0.94	1.20	**0.71**	2.09	1.12	1.55
Max.	**4.12**	7.46	8.43	10.17	5.96	7.11	4.85	12.98	7.62	10.92
Min.	**1.87**	2.02	2.14	2.41	1.89	2.28	2.22	3.80	2.77	2.77

Note. *3 variations:RIAV, RIIV, and RIFV. **4 variations: 3 variations+PWV.

Possible factors that lead to accuracy errors may be: The different wearing condition (position or style) between subjects can be one of the reasons, since the contact between sensor and skin may affect signal received. And the different physiological condition between subjects may also cause different respiratory modulated in these RR features. The use of instant RR estimate method can specifically track the change rate along each respiratory cycle, but the four RR features may have different latency time responses to respiratory activity. Some subjects are more obvious, while some are relatively less obvious. If the

latency is not obvious, it will not affect the fusion results. Instead, this will lead to addition estimation error. This study also found that PWV, the variation of PPG pulse width, performs better accuracy comparing with the other three respiratory-induced variations (as shown in Table 1. Hence while the four RR features are inconsistent, the KF mostly selects the state of PWV as the final RR estimation (as shown in Fig. 4 to Fig. 5). This also proves that PWV has better robustness among the four variations.

6 Conclusions

PPG signals are very easily disturbed by the artifacts, resulting in the difficulty of using PPG for respiratory rate estimation. The proposed model based on KF adaptively fuses four RR feature sequences which derived from the four respiratory-induced variations in noisy PPG. The KF model is formulated by utilizing the relationship of inter-feature coherence and individual feature variations to identify the measurement and state process of the KF model respectively. The quantity of inter-feature divergence and the frequency/amplitude instant variation of the RR feature sequences are utilized to estimate measurement and state process noise covariance, respectively. The KF will accordingly find the optimum estimated state. The final RR estimation is obtained by adaptively fusing estimated RR states of the KF according to the consistency level of the four RR features. The experimental results show that the proposed adaptive feature fusion approach can significantly improve the accuracy of RR estimation using PPG.

Acknowledgements

This work was supported in part by the Ministry of Science and Technology, Taiwan, under Grant MOST103-2923-E006-001-MY3.

References

[1] C.A. Alvarez, C.A. Clark, S. Zhang, E.A. Halm, J.J. Shannon, C.E. Girod, L. Cooper, R. Amarasingham, Predicting out of intensive care unit cardiopulmonary arrest or death using electronic medical record data, BMC Medical Informatics and Decision Making 13(28)(2013).

[2] C.K. Wu, P.C. Chung, C.J. Wang, Representative segment-based emotion analysis and classification with automatic respiration signal segmentation, IEEE Transactions on Affective Computing 13(4)(2012) 482-495.

[3] R.W. Picard, E. Vyzas, J. Healey, Toward machine emotional intelligence: analysis of affective physiological state, IEEE Transactions on Pattern Analysis and Machine Intelligence 23(10)(2001) 1175-1191.

[4] Y.D. Lin, W.T. Liu, C.C. Tsai, W.H. Chen, Coherence analysis between respiration and PPG signal by bivariate AR model, World Academy of Science, Engineering and Technology 3(5)(2009) 1168-1173.

[5] K. Nakajima, T. Tamura, T. Ohta, H. Miike, P. Oberg, Photoplethysmographic measurement of heart and respiratory rates using digital filters, in: Proc. the 15th Annual International Conference of the IEEE Engineering in Medicine and Biology Society, 1993.

[6] L.G. Lindberg, H. Ugnell, P.Å. Öberg, Monitoring of respiratory and heart rates using a fibre-optic sensor, Medical and Biological Engineering and Computing 30(5)(1992) 533-537.

[7] P. Leonard, N.R. Grubb, P.S. Addison, D. Clifton, J.N. Watson, An algorithm for the detection of individual breaths from the pulse oximeter waveform, Journal of Clinical Monitoring and Computing 18(5-6)(2004) 309-312.

[8] P.S. Addison, J.N. Watson, M.L. Mestek, R.S. Mecca, Developing an algorithm for pulse oximetry derived respiratory rate (RR): A healthy volunteer study, Journal of Clinical Monitoring and Computing 26(1)(2012) 45-51.

[9] J. Li, J. Jin, X. Chen, W. Sun, P. Guo, Comparison of respiratory-induced variations in photoplethysmographic signals,

Physiological Measurement 31(3)(2010) 415-425.

[10] A. Johansson, Neural network for photoplethysmographic respiratory rate monitoring, Medical and Biological Engineering and Computing 41(3)(2003) 242-248.

[11] T. Tamura, Y. Maeda, M. Sekine, M. Yoshida, Wearable photoplethysmographic sensors—past and present, Electronics, 3(2014) 282-302.

[12] W. Karlen, S. Raman, J.M. Ansermino, G.A. Dumont, Multiparameter respiratory rate estimation from the photoplethysmogram, IEEE Transactions on Biomedical Engineering 60(7)(2013) 1946-1953.

[13] C. David, J. Graham, P.S. Addison, J.N. Watson, Measurement of respiratory rate from the photoplethysmogram in chest clinic patients, Journal of Clinical Mon. and Comp 21(2007) 51-61.

[14] M.A.F. Pimentel, A.E.W. Johnson, P.H. Charlton, D. Birrenkott, P.J. Watkinson, L. Tarassenko, D.A. Clifton, Towards a robust estimation of respiratory rate from pulse oximeters, IEEE Transactions on Biomedical Engineering 64(8)(2017) 1914-1923.

[15] J. Lazaro, E. Gil, R. Bailon, A. Minchole, P. Laguna, Deriving respiration from photoplethysmographic pulse width, Medical & Biological Engineering & Computing 51(1-2)(2013) 233-242.

[16] W. Karlen, J.M. Ansermino, G. Dumont, Adaptive pulse segmentation and artifact detection in photoplethysmography for mobile applications, in: Proc. 2012 Annual International Conference of the IEEE Engineering in Medicine and Biology Society, 2012.

[17] R.A. Cernat, C. Ungureanu, R.M. Aarts, J.B.A.M. Arends, Real-time extraction of the respiratory rate from photoplethysmographic signals using wearable devices, in: Proc. European Conference on Ambient Intelligence, 2014.

[18] C. Fischer, B. Domer, T. Wibmer, T. Penzel, An algorithm for real-time pulse waveform segmentation and artifact detection in photoplethysmograms, IEEE Journal of Biomedical and Health Informatics 21(2)(2017) 372-381.

[19] S. Nemati, A. Malhotra, G.D. Clifford, Data fusion for improved respiration rate estimation, EURASIP Journal on Advances in Signal Processing 2010(2010) 1-11.

[20] J. Weng, Z. Ye, J. Weng, An improved pre-processing approach for photoplethysmographic signal, in: Proc. 2005 IEEE Engineering in Medicine and Biology 27th Annual Conference, Shanghai, 2005.

[21] K.V. Madhav, M.R. Ram, E.H. Krishna, K.N. Reddy, K.A. Reddy, Use of multi scale PCA for extraction of respiratory activity from photoplethysmographic signals, in: Proc. 2012 IEEE International Instrumentation and Measurement Technology Conference Proceedings, 2012.